

# The Study of Poly(styrene-*co-p*-(hexafluoro-2-hydroxyisopropyl)- $\alpha$ -methylstyrene)/Poly(ethylene oxide) Blends

Shiming Chen, Furong Qiu, Li Tan

Center of Analysis and Measurement, Fudan University, Shanghai 200433, China

Received 26 July 2003; accepted 19 December 2003

**ABSTRACT:** Different hydroxyl content poly(styrene-*co-p*-(hexafluoro-2-hydroxyisopropyl)- $\alpha$ -methylstyrene) [PS(OH)-X] copolymers were synthesized and blends with 2,2,6,6-tetramethyl-piperdine-1-oxyl end spin-labeled PEO [SLPEO] were prepared. The miscibility behavior of all the blends was predicted by comparing the critical miscible polymer-polymer interaction parameter ( $\chi_{crit}$ ) with the polymer-polymer interaction parameter ( $\chi$ ). The micro heterogeneity, chain motion, and hydrogen bonding interaction of the blends were investigated by the ESR spin label method. Two spectral components with different rates of motion were observed in the ESR composite

spectra of all the blends, indicating the existence of microheterogeneity at the molecular level. According to the variations of ESR spectral parameters  $T_a$ ,  $T_d$ ,  $\Delta T$ ,  $T_{50G}$  and  $\tau_c$ , with the increasing hydroxyl content in blends, it was shown that the extent of miscibility was progressively enhanced due to the controllable hydrogen bonding interaction between the hydroxyl in PS(OH) and the ether oxygen in PEO. © 2004 Wiley Periodicals, Inc. *J Appl Polym Sci* 92: 2312–2317, 2004

**Key words:** ESR; spin label; polymer blend; microheterogeneity; miscibility

## INTRODUCTION

Polymer blending is an economic and quick alternative for obtaining materials with optimized properties. The phase morphology and miscibility of polymer blends are of great interest from both academic and industrial points of view. Hydrogen bonding is the most important specific interaction for promoting polymer miscibility.<sup>1–3</sup>

The spin label method, based on electron spin resonance (ESR) spectroscopy, has proved to be powerful in investigating the phase heterogeneity and chain motion of polymer blends.<sup>4–7</sup> Nitroxide radical covalently bonded to polymer chains (spin label) is sensitive to the environment and it can be applied to investigate the structural and motional heterogeneity on a nanoscale length (<5 nm).<sup>8,9</sup> Thus, the method can probe intermolecular specific interaction, at the segmental scale, and extent of miscibility at the molecular scale.

The Hildebrand solubility parameter concept has been used to predict the miscibility of polymer blends.<sup>10</sup> For those blends, with specific interaction between component polymers there is a simple balance between unfavorable physical forces, described in terms of nonhydrogen bonded solubility parameters, and favorable specific interactions. In essence, the

closer the match of the two solubility parameters, the greater the relative strength of the potential intermolecular interaction between the polymeric components of the blend and the greater the probability of miscibility.<sup>11</sup>

In the investigated poly(styrene-*co-p*-(hexafluoro-2-hydroxyisopropyl)- $\alpha$ -methylstyrene)/poly(ethylene oxide) [PS(OH)/PEO] blends, the controllable hydrogen bonding, between the ether oxygen in PEO and the hydroxyl group in PS(OH), was expected to increase the miscibility of the two component polymers progressively. Two main objectives of this work were as follows. First, miscibility behavior of the blend system was predicted based on the Hildebrand solubility parameter concept. The ESR spin label method then was adopted to investigate microheterogeneity, intermolecular hydrogen bonding interaction, and miscibility of the blends.

## EXPERIMENTAL

### Materials

#### SLPEO

2,2,6,6-Tetramethyl-piperdine-1-oxyl end spin-labeled PEO (SLPEO) was prepared according to the method described in our previous paper.<sup>12</sup> The  $M_w$  of SLPEO was 10,000.

#### PS(OH)

PS(OH), with different contents of hydroxyl-containing units, was copolymerized by styrene and

Correspondence to: S. Chen (smchen@fudan.edu.cn).

TABLE I  
Characterization Data for PS(OH)-X Copolymers

Polymer <sup>a</sup>	$M_n \times 10^{-4}$	$M_w/M_n$	OH content (mol%)
PS(OH)-2	2.0	1.60	1.67
PS(OH)-5	2.4	1.73	4.88
PS(OH)-8	1.6	1.65	8.22
PS(OH)-12	1.9	1.50	11.66
PS(OH)-20	1.8	1.68	19.41
PS(OH)-27	1.4	1.74	27.28

<sup>a</sup> The number following PS(OH) represented the approximate integer value of the molar content of HFMS in the copolymer.

*p*-(hexafluoro-2-hydroxylisopropyl)- $\alpha$ -methylstyrene (HFMS) as discussed previously.<sup>13,14</sup> In PS(OH)-X, X was the mole content of hydroxyl groups in the copolymer. The characterization data for the PS(OH) copolymers are listed in Table I. The chemical structures of SLPEO and PS(OH) are listed in Figure 1.

### Preparation of blends

Weight ratio blends (1 : 3) of SLPEO to different hydroxyl content PS(OH) copolymer were prepared by mixing their respective 3% solutions in benzene. After the solvents were evaporated, the blends were dried for 3 days under vacuum at 323 K. The notation used for PS(OH)-X/SLPEO blends is PP-X, where X is the mole content of hydroxyl group in the copolymer.

### ESR measurements

ESR spectra were measured at the X band with a Bruker 200D-SRC spectrometer operating at 9.67 GHz and 100 KHz modulation. An Aspect 3000 computer, with EPR3002 software controlled data acquisition. ESR spectra, as a function of temperature, were measured with the Bruker ER4111VT variable temperature unit. All the blend samples were allowed to equilibrate for at least 5 min after approaching the corresponding temperature. The microwave power (2 mW) and modulation amplitude (1 G) were adjusted well below saturation and distortion of the spectra.

## RESULTS AND DISCUSSION

### Interaction parameter ( $\chi$ ) calculation and miscibility prediction

Coleman and coworkers<sup>11</sup> have rationalized the phase behavior, and other thermodynamic properties, of binary mixtures of polymers by expressing the free energy of mixing as

$$\frac{\Delta G_M}{RT} = \frac{\Phi_A \ln \Phi_A}{N_A} + \frac{\Phi_B \ln \Phi_B}{N_B} + \chi \Phi_A \Phi_B + \frac{\Delta G_H}{RT} \quad (1)$$

Where  $\Phi_A$ ,  $\Phi_B$ ,  $N_A$ , and  $N_B$  are, respectively, the volume fraction and degree of polymerization of polymers A and B,  $\chi$  is the polymer-polymer interaction parameter representing physical forces only, while the  $\Delta G_H$  term reflects the free energy changes corresponding to the specific interactions, such as hydrogen bonding.  $\chi$  can be related to the Hildebrand solubility parameters of the component polymers.<sup>15</sup>

$$\chi = \frac{V_r}{RT} (\delta_A - \delta_B)^2 \quad (2)$$

Where  $V_r$  is the reference molar volume and  $\delta_A$  and  $\delta_B$  are the solubility parameters of polymers A and B. For simplicity, in the PS(OH)-X/PEO blend system, we denote PS(OH)-X and PEO as A and B instead of using the full names.

The two separate solubility parameters,  $\delta_A$  and  $\delta_B$ , for PS(OH)-X and PEO in eq.(2) can be calculated by a progressed solubility parameter concept which incorporates three individual contributions to the total solubility parameter:  $\delta_d$  (contribution of dispersion forces),  $\delta_p$  (contribution of polar forces), and  $\delta_h$  (contribution of hydrogen bonding forces).<sup>10</sup>

$$\delta = \sqrt{\delta_d^2 + \delta_p^2 + \delta_h^2} \quad (3)$$

The component solubility parameter of  $\delta_{dA}$ ,  $\delta_{pA}$ , and  $\delta_{hA}$  for  $\delta_A$  is given by the linear combination of the solubility parameters of the two monomers (HFMS and styrene) in the copolymer.<sup>10</sup>

Component solubility parameters ( $\delta_d$ ,  $\delta_p$ , and  $\delta_h$ ) were calculated, in a consistent manner, by using the group molar attraction constants and group molar volume of Hansen compiled by Van Krevelen.<sup>16</sup> The calculated  $\delta_{dA}$ ,  $\delta_{pA}$ , and  $\delta_{hA}$  values in PS(OH)-X copolymer and  $\delta_{dB}$ ,  $\delta_{pB}$ , and  $\delta_{hB}$  values in PEO are listed in Table II. According to  $\delta_{dA}$ ,  $\delta_{pA}$ , and  $\delta_{hA}$  and  $\delta_{dB}$ , and  $\delta_{hB}$  values, the solubility parameters of  $\delta_{PS(OH)-X}$  and  $\delta_{PEO}$ , calculated using eq.(3), are plotted in Figure 2 as a function of hydroxyl content in the PS(OH)-X copolymer. Thus the value of  $\chi$  for the PP-X blends may now be determined according to eq.(2), where the

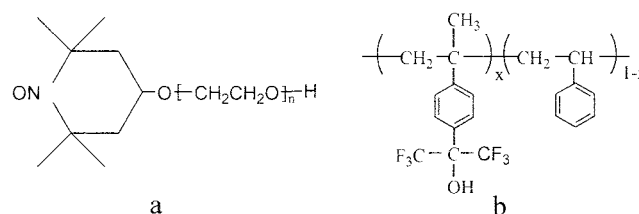


Figure 1 Chemical structures of (a) SLPEO and (b) PS(OH).

TABLE II  
Calculated Component Solubility Parameter  
Values for  $\delta_A$  and  $\delta_B$

PS(OH)-X	$\delta_{dA}$	$\delta_{pA}$	$\delta_{hA}$
PS(OH)-2	20.35	1.49	1.63
PS(OH)-5	20.39	1.74	1.83
PS(OH)-8	20.43	1.98	2.03
PS(OH)-12	20.49	2.31	2.30
PS(OH)-20	20.60	2.96	2.83
PS(OH)-27	20.70	3.53	3.30
PEO	$\delta_{dB} = 21.06$	$\delta_{pB} = 11.11$	$\delta_{hB} = 7.99$

molar volume of the PS(OH)-X repeat was employed as the reference volume,  $V_r$ . The results are summarized in Figure 3. The value of  $\chi_{PP-X}$  was determined by two factors: the size of the reference volume  $V_r$ , which increased with increasing HFMS content in the PS(OH)-X copolymer, and the difference in the solubility parameter of PS(OH)-X,  $\delta_A$ , and its value relative to  $\delta_B$ , the solubility parameter of PEO. From Figure 3 it is known that  $\chi_{PP-X}$  decreased with increasing hydroxyl content in PS(OH)-X copolymer. A review of the polymer-polymer interaction parameter  $\chi_{crit}$  sets the upper limit for miscibility across the entire composition range.<sup>11</sup>

$$\chi_{crit} = \frac{1}{2} \left[ \frac{1}{N_A^{0.5}} + \frac{1}{N_B^{0.5}} \right]^2 \quad (4)$$

$N_A$  and  $N_B$  are the degrees of polymerization of polymers A and B. Coleman and coworkers<sup>11</sup> have provided a summary of the upper limits of the critical values of the solubility parameter difference  $\Delta\delta_{crit} = |\delta_A - \delta_B|$  as a function of different kinds of interactions, such as weak hydrogen bonds, moderate hydro-

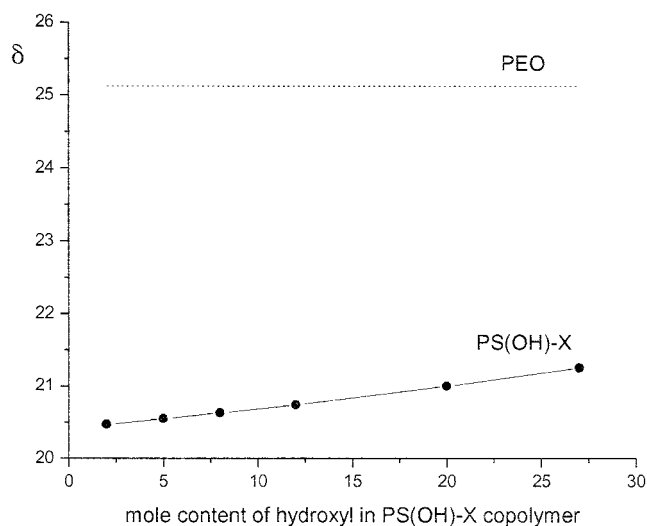


Figure 2 Calculated values of the solubility parameter for PS(OH)-X copolymer.

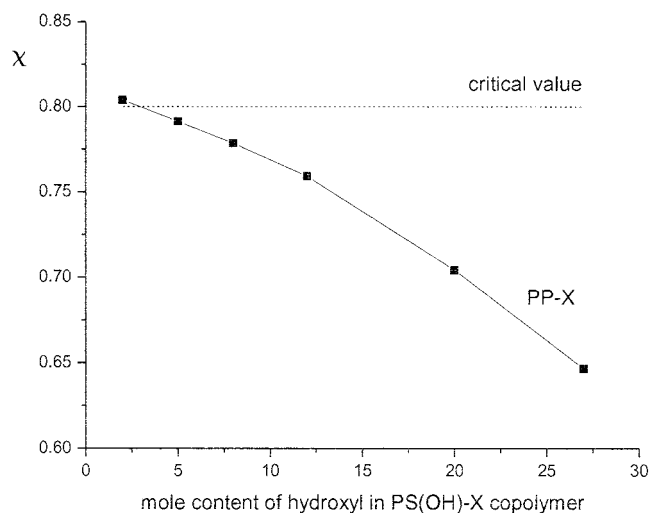


Figure 3 Calculated values of  $\chi$  for PP-X blends.

gen bonds, and strong hydrogen bonds. Simply put, the presence of such favorable intermolecular interactions effectively increases the magnitude of  $\chi_{crit}$  and permits the tolerance of a greater difference in the nonhydrogen bonding solubility parameters of the two polymers,  $\Delta\delta$ . In the PS(OH)-X/PEO blends, the outstanding strength of the hydrogen bonding, between the hydroxyl linked with strong proton-donating units  $[(CF_3)_2(OH)C-]$  in PS(OH) and ether oxygen in PEO, shows they can be included in the strong hydrogen bonding type.<sup>11</sup> Employing the  $\chi_{crit}$  value of 0.8 for the blend with strong hydrogen bonding,<sup>11</sup> the phase behavior of PP-X blends can be predicted. If  $\chi_{PP-X}$  is more than  $\chi_{crit}$ , the blend is immiscible; if  $\chi_{PP-X}$  is less than  $\chi_{crit}$ , the blend is miscible. A  $\chi_{crit}$  of 0.8 leads to a prediction that PEO should be miscible with PS(OH) copolymers containing about 2% or greater hydroxyl content.

### Microheterogeneity and miscibility

#### Fast motion component fraction ( $F\%$ )

The temperature dependence of ESR spectra for all the spin-labeled PP-X blends were measured in the temperature range of 100~420 K. Selected ESR spectra for PP-5 and PP-20 blends are presented in Figures 4 and 5. At low temperatures the spectra of all the blends were predominantly composed of the broad line, slow motion component. As the temperature was increased above a specific value, a fast motion component appeared, simultaneously existing with the slow motion component. When the temperature was further increased, the intensity of the fast motion component in the composite spectrum increased at the expense of the slow motion component. In the end, the slow motion component disappeared and the spectrum was composed entirely of the fast motion component.

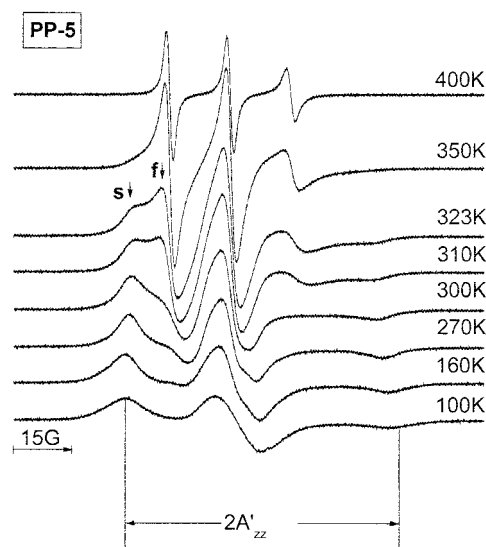


Figure 4 ESR spectra of SLPEO in PP-5.

Observation of the slow and the fast motion (illustrated by "s" and "f" at low field in Figs. 4 and 5) indicated that the SLPEO segments existed in two dynamically different molecular environments due to the local heterogeneity in the blends: a PEO-rich microdomain and a PS(OH)-rich microdomain.<sup>17-19</sup> In the PEO-rich domain, the environment was more flexible and the SLPEO segment motion was faster, while in the PS(OH)-rich domain, the environment was more rigid and the SLPEO segment motion was slower.

Although the relative fast or slow motion component intensity was not an absolute measure, for the number of immobilized or freely rotating spin label located in the more rigid microdomain or the more flexible microdomain, due to the simplicity of quantitative analysis, the fast motion component fraction noted by  $F\%$  can be estimated from the ratio of the intensity of the fast motion in the composite spectrum

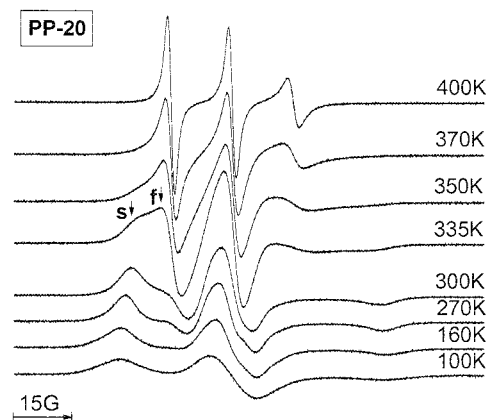


Figure 5 ESR spectra of SLPEO in PP-20.

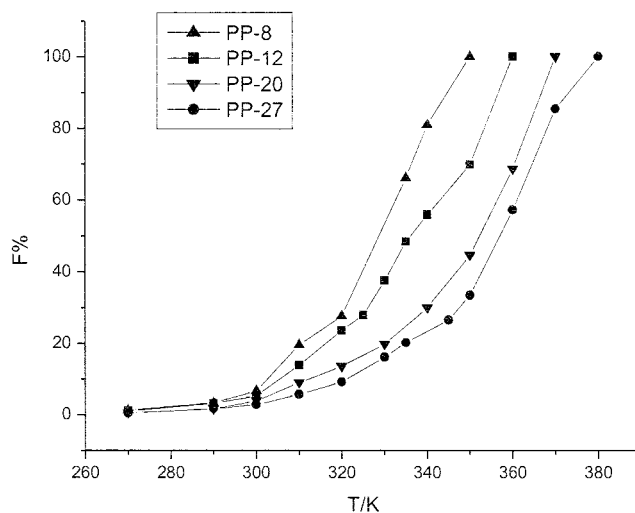


Figure 6 Change of fast motion fraction ( $F\%$ ) with temperature.

to that of the fast motion in the wholly single spectrum.<sup>20</sup> The fast component fraction, obtained by this method is illustrated in Figure 6 for selected PP-X blends. Figure 6 shows that, as the temperature was raised, the fast motion component increased at the expense of the slow motion component. The relative number of segregation of the probe molecules in flexible and rigid microdomains can also be obtained from  $F\%$  and  $(1-F)\%$  quantitatively.

#### $T_a$ , $T_d$ , and $\Delta T$

The composite ESR spectra of all PP-X blends that evolved in a certain temperature range appear to be the most valuable contribution of the spin label method to differentiate more than one phase: phase heterogeneity on molecular level. The PP-X blends were partially miscible and the two component polymer chains penetrated together via the hydrogen bonding interaction between the hydroxyl in PS(OH) and the ether oxygen in PEO. From PP-2 to PP-27, the miscibility extent between the two component polymers has been progressively enhanced by controllable hydrogen bonding interaction. And this miscibility enhancement can be deduced from three temperature parameters:  $T_a$ ,  $T_d$ , and  $\Delta T$ ,  $T_a$  is the temperature when the fast motion component appeared,  $T_d$  is the temperature when the slow motion component disappeared, and  $\Delta T$  is the span between  $T_a$  and  $T_d$ . The  $T_a$ ,  $T_d$ , and  $\Delta T$  values for all the PP-X blends are listed in Table III. Table III showed that  $T_a$ s were the same for all PP-X blends while  $T_d$  and  $\Delta T$  increased with the increasing hydroxyl content in the PS(OH)-X copolymer. The same  $T_a$  values in different hydroxyl content blends indicated that the appearance of fast motion was not sensitive to polymer matrix rigidity. It was



TABLE III  
 $T_a$ ,  $T_d$ , and  $\Delta T$  Values for PP-X Blends

	PP-2	PP-5	PP-8	PP-12	PP-20	PP-27
$T_a$ (K)	270	270	270	270	270	270
$T_d$ (K)	340	350	355	360	370	380
$\Delta T$ (K)	70	80	85	90	100	110

assumed that, in the low temperature (<270 K), the motion of spin label molecules was not much influenced by the surrounding polymer matrix.<sup>21</sup> Below 270 K, both PEO and PS(OH) chains were in the glass state for all the PP-X blends. The spin label molecules rotated in the "holes" of dimensions comparable to those of a label in the polymer matrix and were almost independent of the molecular motion of the polymer. When the temperature was raised, both polymer chains were activated. The spin label motion was perturbed by the molecular motion of the polymer chains. With the progressively increasing hydrogen bonding interaction, the penetration of one kind of polymer chain into the other polymer domain became more and more profound. Accordingly the mesh size of the physical network, induced by hydrogen bonding cross-linking, progressively decreased.<sup>22</sup> So a higher temperature and a broader temperature range were needed to obtain the completely narrowed ESR spectra.

$T_{50G}$  and  $\tau_c$

The physical cross-linking enhancement promoted the matrix rigidity of the polymer blend progressively, which could be substantiated from the  $T_{50G}$  change:  $T_{50G}$  is the temperature at which the separation of the

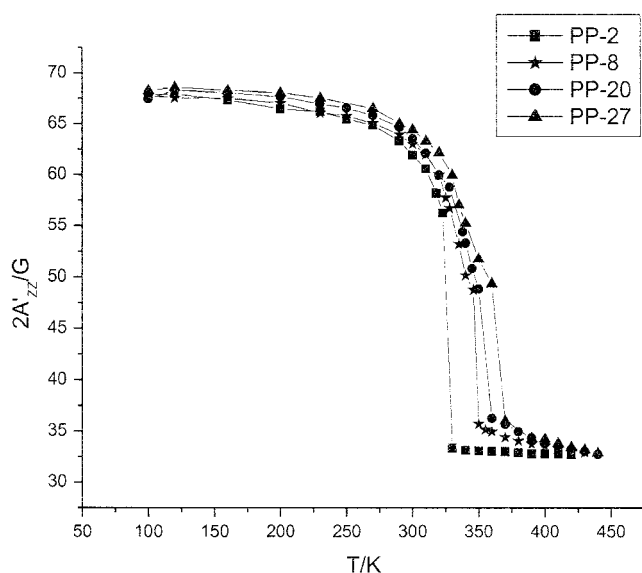


Figure 7 Temperature dependence of  $2A'_{zz}$ .

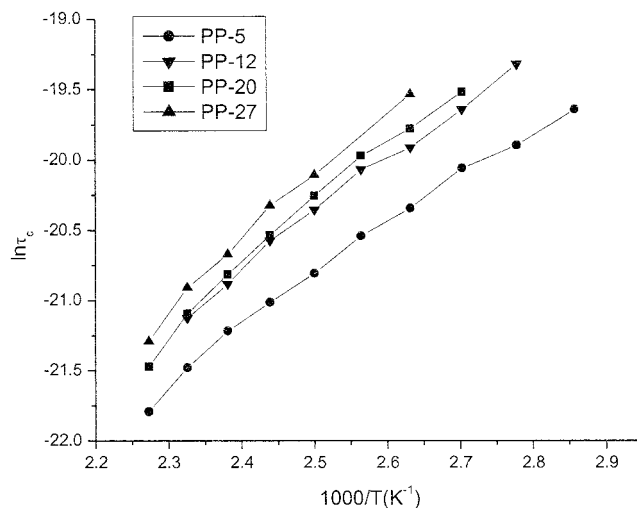


Figure 8 Variation of  $\ln\tau_c$  with the reciprocal temperature.

outermost peaks ( $2A'_{zz}$ ) (measured in the manner shown in Fig. 4) of the ESR spectrum of stable free nitroxide radicals in polymer matrix is 50 G.<sup>23</sup> It is a convenient parameter for comparing the environments of the spin label.  $T_{50G}$  can be regarded as a high frequency  $T_g$ , where a higher value of  $T_{50G}$  indicates a stiffer environment.<sup>24</sup> For selected PP-X blends the plot of  $2A'_{zz}$  as a function of temperature, is shown in Figure 7. The  $T_{50G}$  values for PP-2, PP-8, PP-20, and PP-27 blends are 323, 340, 350, and 360 K, respectively. It is obvious that  $T_{50G}$  increased with the increasing hydroxyl content in PS(OH)-X copolymer, which proves the progressively improved matrix rigidity in the polymer blend.<sup>22</sup>

On the other hand, the progressively enhanced net-like interconnection in polymer blends would also contribute to the motional restriction of polymer segments, which could be characterized by the rotational correlation time,  $\tau_c$ .<sup>25</sup>

$$\tau_c = 6.6 \times 10^{-10} \left[ \left( \frac{h_0}{h_{-1}} \right)^{1/2} - \left( \frac{h_0}{h_{+1}} \right)^{1/2} \right] \times \Delta H_{PP} \quad (5)$$

Where  $h_{+1}$ ,  $h_0$ , and  $h_{-1}$  are the measured low, central, and high field peak-to-peak amplitudes of the nitroxide radical spectrum;  $\Delta H_{PP}$  is the width of the central peak in Gauss.

$\tau_c$  can quantitatively characterize the changes in the rotational rate of the nitroxide spin label. The natural logarithm of  $\tau_c$  in the fast motion range ( $10^{-9}$  s <  $\tau_c$  <  $10^{-11}$  s), as a function of the reciprocal temperature, is shown in Figure 8. The change of  $\tau_c$  shows the enhanced hydrogen bonding interaction in the blends restricted the motion of the spin probe progressively.  $\tau_c$  decreased with increasing temperature for any PP-X blend, while it increased with increasing hydroxyl content in the PS(OH)-X at any temperature.

### CONCLUSION

By comparing the critical miscible polymer–polymer interaction parameter ( $\chi_{\text{crit}}$ ) 0.8 with the polymer–polymer interaction parameter ( $\chi$ ), a prediction is given that PEO could be miscible with PS(OH) copolymers containing about 2% or more hydroxyl content.

For all the spin-labeled blends, two spectral components with different rates of motion, fast and slow, were observed in a different temperature range of the ESR spectra. The difference between motion rates indicated the existence of microheterogeneity at the molecular level: the faster one corresponded to nitroxide radical motion trapped in the PEO-rich microdomain and the slower one corresponded to nitroxide radical motion trapped in the PS(OH)-rich microdomain.

According to the variation of ESR spectral parameters  $T_a$ ,  $T_d$ ,  $\Delta T$ ,  $T_{50G}$ , and  $\tau_c$  with hydroxyl content in blends, it can be concluded that the scale of miscibility was progressively enhanced due to the increasing hydrogen bonding interaction between the hydroxyl in PS(OH) and the ether oxygen in PEO.

### References

1. Utracki, L. A. *Polymer Alloy and Blends*. Hanser: Munich, 1989.
2. Coleman, M. M.; Graf, J. F.; Painter, P. C. *Specific Interactions and the Miscibility of Polymer Blends*. Technomic: Lancaster PA, 1991.
3. Paul, D. R.; Bucknall, C. *Polymer Blends*. J Wiley: New York, 2000; vols. I and II.
4. Culin, J.; Frka, S.; Andreis, M. *Polymer* 2002, 43, 3891.
5. Varghese, B.; Schlick, S. *J Polym Sci Part B* 2002, 40, 415.
6. Andreis, M.; Rakvin, B.; Veksli, Z.; Rogosic, M.; Mencer, H. J. *Polymer* 1999, 40, 1955.
7. Schlick, S.; Harvey, Alonso-Amigo, M. G.; Klempner, D. *Macromolecules* 1989, 22, 822.
8. Veksli, Z.; Andreis, M.; Rakvin, B. *Prog Polym Sci* 2000, 25, 949.
9. Muller, G.; Stadler, R. *Macromolecules* 1994, 27, 1551.
10. David, D. J.; Sincock, T. F. *Polymer* 1992, 33, 4505.
11. Coleman, M. M.; Serman, C. J.; Bhagwagar, D. E.; Painter, P. C. *Polymer* 1990, 31, 1187.
12. Jin, G. D.; Tan, L.; Chen, S. M.; Yan, X. M.; Shen, Y. M. *Chin J Magn Reson* 2001, 18, 13.
13. Jiang, M.; Chen, W.; Yu, T. *Polymer* 1991, 32, 984.
14. Qiu, X.; Jiang, M. *Polymer* 1994, 35, 5084.
15. Balazs, A. C.; Sanchez, I. C.; Epstein, I. R.; Karasz, F. E.; MacKnight, W. J. *Macromolecules* 1985, 18, 2188.
16. Van Krevelen, D. W. *Properties of Polymers*. Elsevier: Amsterdam, 1976.
17. Muller, G.; Stadler, R. *Macromolecules* 1994, 27, 1551.
18. Muller, G.; Stadler, R.; Schlick, S. *Makromol Chem Rapid Commun* 1992, 13, 117.
19. Pilar, J.; Sikora, A.; Labsky, J.; Schlock, S. *Macromolecules* 1993, 26, 137.
20. Shimada, S.; Hori, Y.; Kashiwabara, H. *Macromolecules* 1992, 25, 2771.
21. Tan, L.; Chen, S. M.; Ping, Z. H.; Shen, Y. M. *Magn Reson Chem* 2003, 41, 481.
22. Tan, L.; Chen, S. M.; Ping, Z. H.; Shen, Y. M. *Polym Int* 2004, 53, 204.
23. Tormala, P.; Weber, G. *Polymer* 1978, 19, 1026.
24. Cameron, G. G.; Stewart, D. *Eur Polym J* 1993, 29, 245.
25. Kivelson, D. J. *J Chem Phys* 1960, 33, 1107.